

In vivo anti-tumor and anti-metastatic activity of renieramycin M and doxorubicin combination treatments on 4T1 breast cancer murine model

Zildjian G. Acyatan, Shalice R. Susana-Guevarra, Myra Ruth D. Picart, Eliza L. Belen, Lilibeth A. Salvador-Reyes, and Gisela P. Concepcion*

The Marine Science Institute, College of Science, University of the Philippines, Diliman, Quezon City 1101, Philippines

ABSTRACT

Breast cancer continues to be a serious global health concern, necessitating novel treatment approaches. This study explores the potential of combination therapies, investigating the combinatorial effects of doxorubicin (Dox) and renieramycin M (RM) *in vivo*, previously shown to have synergistic effects *in vitro*. Single drug administrations and combination treatments were tested on *in vivo* breast cancer murine models using 4T1-injected BALB/c mice. Tumor volume, animal mortality, and clinical toxicity were monitored, and *in silico* toxicity assessment was performed. Histopathological analyses using hematoxylin and eosin (H&E) staining, and immunohistochemistry utilizing the p63 breast cancer marker were used for validation. The combination treatment of Dox and RM (5 mg/kg + 1 mg/kg) displayed a 46.53% reduction in tumor volume and an 83.63% decrease in observed metastatic infiltration in the liver. Furthermore, the combination treatment of Dox and RM significantly delayed and reduced the clinical signs of toxicity, as revealed by the decline in observed mortality as opposed to animal deaths in single drug

treatments. Our study highlights the potential synergism between Dox and RM as combination therapy for breast cancer treatment. These findings provide possible strategies to improved therapies, offering a more effective and less toxic approach to mitigating breast cancer.

INTRODUCTION

Breast cancer is still the most common cancer in women, accounting for the second most common cause of cancer death (Arnold et al. 2022). An estimated 30–75% of patients undergoing surgery and adjuvant treatment will develop recurrent metastatic disease (Gogate et al. 2021; Mariotto et al. 2011). Metastatic breast cancer (MBC) is essentially incurable with standard therapy and patients with MBC have a median survival of about 2 years after detection of metastasis (Gamucci et al. 2007). Doxorubicin (Dox) is an anthracycline drug (Figure 1) widely used in chemotherapy regimens for patients with MBC and has shown overall response rates of 35%–50% in patients with MBC who have not previously received chemotherapy (Andreopoulou and Sparano 2013; Zheng et al. 2015). Despite its excellent anti-tumor activity, Dox has a relatively low

*Corresponding author

Email Address: gpconcepcion@gmail.com

Date received: April 19, 2024

Date revised: August 19, 2024

Date accepted: August 20, 2024

DOI: <https://doi.org/10.54645/202417SupNLT-14>

KEYWORDS

Breast cancer, doxorubicin, renieramycin M, combinatorial therapies, synergism

therapeutic index, and its clinical utility is limited due to acute and chronic toxicities such as myelosuppression, immunosuppression, and dose-cumulative cardiotoxicity (Chatterjee et al. 2010; Dulf et al. 2023). Therefore, combination treatment with another highly effective novel non-toxic drug that can lower the dose of chemotherapeutic agents would be desirable (Meco et al. 2003).

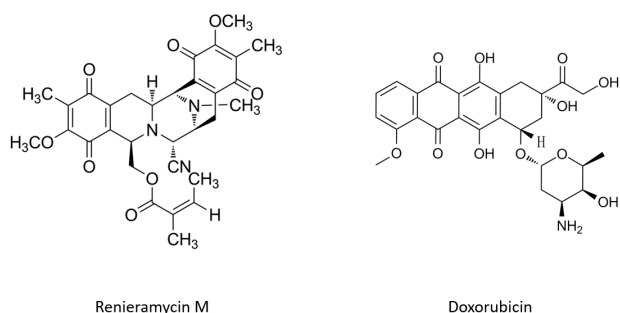


Figure 1: Chemical structures of renieramycin M and doxorubicin

Renieramycin M (RM) is a marine natural product tetrahydroisoquinoline purified from the blue sponge *Xestospongia* sp. with bioactivity that has been associated with nanomolar level IC_{50} cytotoxicity on various cancer cell lines: colon, lung, melanoma, pancreatic, and breast cancer cells (Charupant et al. 2009; Charupant et al. 2009; Saito et al. 2004; Suwanborirux et al. 2003; Tun et al. 2019) (Figure 1). Several mechanisms of action have been proposed for RM. This includes inhibition of the PIK3-Akt and ERB pathways, and downregulation of MCL-1, BCL-1, and BRCA1 genes, and targeting focal adhesion in the cell (Chamni et al. 2020; Charupant et al. 2009; Halim et al. 2011; Tun et al. 2019) making RM a potent anti-tumor agent and a good candidate for combination treatment with Dox.

The combination of Dox and RM holds promise as potential anti-tumor and anti-metastatic therapies. In fact, Dox and RM have been demonstrated to have synergistic effects on breast cancer cell lines (Tun et al. 2019). In this report, we performed *in vivo* studies as proof of concept or proof of principle to determine the clinical potential and effectiveness of Dox + RM against breast cancer in a murine model.

MATERIALS AND METHODS

Renieramycin M (RM) used for this study was isolated and purified using the method of Suwanborirux et al. (2003), obtained from the open-sea mariculture of the blue sponge *Xestospongia* sp. in Puerto Galera, Oriental Mindoro (Santiago et al. 2019). RM is > 99% pure. All NMR and MS data agreed with literature values. A 10 mM (5.75 mg/mL) stock solution of RM was prepared in dimethyl sulfoxide (DMSO), and then further diluted to 100 μ M using the same solvent. Doxorubicin (Dox), 98-102% pure (HPLC), was purchased from Sigma-Aldrich Co. (D1515) (Milwaukee, Wisconsin USA) and dissolved in sterile water to make an 8.5 mM (5 mg/mL) solution. Both stock solutions were aliquoted in several tubes, and stored at $-20^{\circ}C$. Further dilutions of RM and Dox were prepared in 10% DMSO and sdH_2O , respectively.

Cell culture

The 4T1 mouse breast adenocarcinoma cells (CRL-2539TM) were acquired from ATCC (American Type Culture Collection) and grown *in vitro* until they reached 60-80% confluency according to manufacturer's protocol. 4T1 cells were maintained at $37^{\circ}C$, 5% CO_2 in RPMI 1640 with 10% FBS (Gibco) and 1%

antibiotics and antimycotics (anti-anti) (Gibco). 4T1 cells were harvested by trypsinization prior to injection to test animals.

Animal Studies and Ethics Statement

All protocols in this manuscript involving the use of animals were approved by the Institutional Animal Care and Use Committee of the University of the Philippines Diliman (#AP-2020-17, approved 4 April 2020; #AP-2022-21, approved 4 November 2022). The 4T1 tumor mouse model is a suitable animal model for metastatic breast cancer (Pulaski and Ostrand-Rosenberg 1998). The animal experiments were performed at the Animal Facility of the Marine Science Institute. Healthy 6-8 week-old female BALB/c mice were used for the experiment. Mice were injected subcutaneously in the mammary pad with 4T1 cells (7,000 cells/50 μ L in PBS). Treatment commenced when the tumor became palpable. All treatments were administered intraperitoneally(). Outlier data points were calculated using the two-dimensional mathematical model and removed from tumor volume analyses (Sápi and Kovács 2015).

Tumor Measurements and Volume Computation

Four mice per treatment cohort were used for the solvent control (1% DMSO in PBS), positive control (Dox at 5 mg/kg concentration) and test samples for each treatment doses (consisting of single drug and combination drug doses). Administration was performed following a 3-day treatment regimen (once-daily dosing) during the entire length of the study. Treatments were introduced intraperitoneally. Tumor growth was measured every day for a period of one month. Tumor volumes and growth rates were calculated as described by Faustino-Rocha et al. (2013). Briefly, two perpendicular dimensions of each tumor were measured using a Vernier caliper, and tumor volumes were calculated using the formula for an ellipsoid: $W \times L \times 0.5$, where width (W) is less than or equal to length (L).

After the said period, the mice were sacrificed with CO_2 . Tumors were dissected, with a portion preserved in 10% buffered formalin for histological evaluation, while the remainder was preserved at $-80^{\circ}C$.

Histopathology and Immunohistochemistry

Extracted tumors preserved in 10% buffered formalin were subjected to sectioning and biopsy. H&E (hematoxylin and eosin) staining and immunohistochemistry using p63 antibody staining were performed by Hi-Precision Diagnostics (Quezon City, Philippines). After the tissue was sectioned and embedded on a glass slide, the samples were stained with H&E using standard protocols. In brief, the slide containing the tissue was deparaffinized by allowing the slide to be flamed several times while placed in xylene. The tissue section was then hydrated by passing through decreasing concentrations of alcohol baths and water (100%, 90%, 80%, 70%). The slide was then stained in hematoxylin for 3-5 min, differentiated in 1% acid alcohol, ammonia water and finally eosin, with washing with tap water in between each staining step. Slides were dehydrated in increasing concentrations of alcohol and cleared in xylene.

The p63 staining (IHC-Tek) was performed following the manufacturer's instructions. In brief, a dilution of 1:200 was performed with an incubation time of 1 h at room temperature. The serum blocking step was not necessary to reduce the background and unspecific staining.

Statistical Analysis

All experiments were performed with at least two to three independent trials. Results were expressed as mean \pm SD or mean \pm SEM. Statistical comparisons were performed using GraphPad PrismTM version 7.03 using one-way ANOVA (analysis of variance) followed by Bonferroni or Dunnett's

Multiple Comparison Test or Tukey's Multiple Comparison Test or unpaired two-tailed Student's *t*-test. $p < 0.05$ were considered significant.

RESULTS AND DISCUSSION

Induction of metastatic breast cancer by inoculation of 4T1 cells

To determine the combinatorial effects of RM and Dox as anti-tumor agents, 6–8-week-old female BALB/c mice were inoculated with 4T1 breast cancer cells to simulate breast cancer tumors in a murine model. The number of cells was optimized by injecting 100, 1,000, 10,000, and 100,000 cells (Supplementary Figure 1). Tumor size was monitored daily by measuring the length and width using a Vernier caliper and calculating the volume as described in the Methods section. (Carlson et al. 2011). A cell count of 7,000 cells was most appropriate to ensure palpable tumors before day seven. Mice that were injected with 10,000 and 100,000 cells showed palpable tumors as early as two days post inoculation, while mice that were injected with $\leq 1,000$ cells displayed palpable tumors more than seven days post inoculation. The introduction of the first treatment was timed one day after more than half of the mice exhibited palpable tumors (Carlson et al. 2011). Mice were then grouped and subjected to different dosage combination treatments. Mice were observed for five weeks before being euthanized. Tumors were successfully grown on each BALB/c mouse, as seen in representative animals in Figure 2.

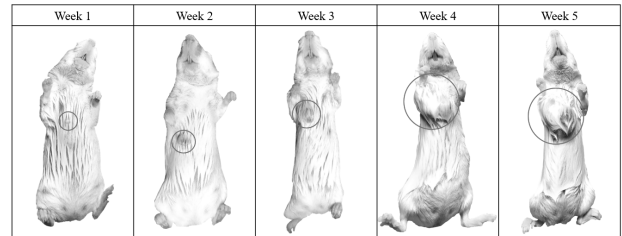


Figure 2: Progression of palpable tumors in mice after inoculation of 4T1 breast cancer cells. BALB/c mice (6–8-weeks old) were injected (s.c) with 4T1 cells (7,000 cells/50 μ L) in their upper right mammary gland. Tumor size was measured daily.

Effects of treatments on tumor volume

The first of the three treatments was administered intraperitoneally once the tumor became palpable, measuring at least 2 x 2 mm. This occurred on the seventh day following inoculation. Subsequently, the second and third treatments were administered on day 10 and day 13, respectively, with a 3-day gap between each treatment. The 3-day interval was decided based on the previously described administration of chemotherapy drugs in murine models, where chemotherapy drugs were administered every other day (Bao et al. 2011) or once every seven days (Argenziano et al. 2020) depending on the class and dosage of drugs introduced. Given the absence of prior reports on the excretion and half-life of the combined Dox and RM *in vivo*, we chose a 3-day interval between treatments as the dosing schedule (Mishima et al. 2005).

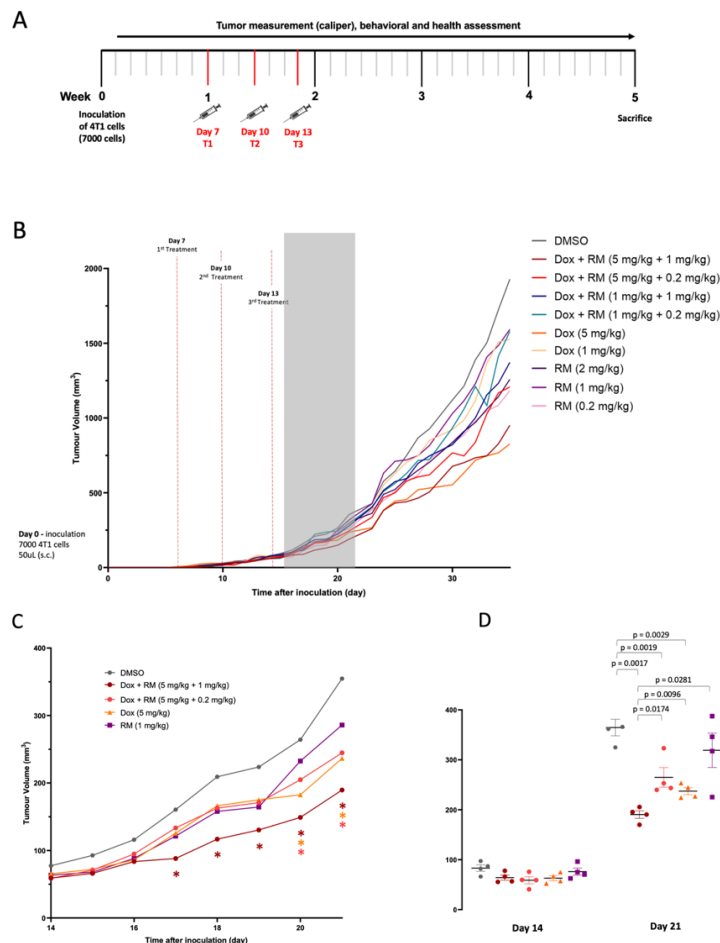


Figure 3: Timeline and progression of tumor volume in BALB/c mice. Combination treatments of Dox + RM, and single-drug treatments were observed to decrease tumor size in primary breast cancer xenografts. BALB/c mice bearing 4T1 cells were treated with multiple doses to determine the effects of Dox + RM combination. A) Schematic diagram of the timeline of inoculation and treatment events. B) Tumor volume and experimental protocol from day 0 to end point day 35 of all treatment setup. C) Tumor volume for setups of specific combination doses and single drug doses that showed the greatest reduction (day 14 to day 21). D) Individual tumor volumes on day 14 and day 21 from the same treatment setups highlighted in B. ($n = 4/group$). Mean \pm SEM, * and bars with p -value mean significant differences among treatments (ANOVA and Tukey's multiple comparison test; $P < 0.05$).

Figure 3 shows the tumor volume for each setup following daily measurements. Tumor volumes were compared against treatment setups and vehicle control (DMSO) across a period of five weeks. The gray bar in Figure 3B highlights the one-week period succeeding the three treatments. Figures 3C and 3D are on four setups: two combination doses (Dox + RM: 5 mg/kg + 1 mg/kg), Dox + RM: 5 mg/kg + 0.2 mg/kg) and single-drug concentrations for Dox (5 mg/kg) and RM (1 mg/kg). We observed a significant reduction (45.10 %) starting on day 17 for the combination treatment Dox + RM (5 mg/kg + 1 mg/kg) compared to the vehicle control setup. This was observed until day 21, where the combination treatment Dox + RM (5 mg/kg + 1 mg/kg) showed a significant reduction of 46.53% compared to vehicle control. The effectiveness of this combination dose was significantly higher compared to the other combination doses as well as the single-dose treatments.

Morbidity and animal survival

The general health condition of each mouse was monitored throughout the course of the experiment. This was done by checking its weight, food intake, and cage activity daily (Supplementary Figure 2). Moribundity and sluggishness were noted as signs of drug toxicity and are often indications of clinical toxicity (Sewell et al. 2015; Yamagishi et al. 2022). The

death of mice for trial 1 (data not shown) and trial 2 are reported in a Kaplan-Meier survival plot (Dudley et al. 2016) in Figure 4. High-dose introduction of Dox (5 mg/kg) caused the greatest number of deaths due to drug toxicity and was expected since Dox has been previously reported to cause late-stage cardiotoxicity and liver toxicity *in vivo* (Chamni et al. 2020; Chatterjee et al. 2010; Dulf et al. 2023). The second group with the greatest number of deaths was from the setup with high-dose RM treatment (1 mg/kg). RM has been reported to have cytotoxic effects *in vitro* in different types of cancer cell lines: non-small cell lung cancer, colon cancer, pancreatic cancer, and breast carcinoma with putative mechanisms targeting the PIK3-Akt and ERB pathways, and downregulation of MCL-1, BCL-1, and BRCA1 genes (Chamni et al. 2020; Charupant et al., 2009; Tun et al. 2019). Interestingly, combination treatments Dox + RM (5 mg/kg + 1 mg/kg and 5mg/kg + 0.2 mg/kg) showed significant reduction in the deaths compared to its counterpart single treatments of the same dosage. Only one death was observed in the Dox + RM (5 mg/kg + 1 mg/kg) and none was observed in the Dox + RM (5 mg/kg + 0.2 mg/kg). The reported death observed in Dox + RM (5 mg/kg + 1 mg/kg) occurred on day 33, while the first observed deaths in single dose treatments were on day 24 and day 29 for Dox (5 mg/kg) and RM (1 mg/kg), respectively.

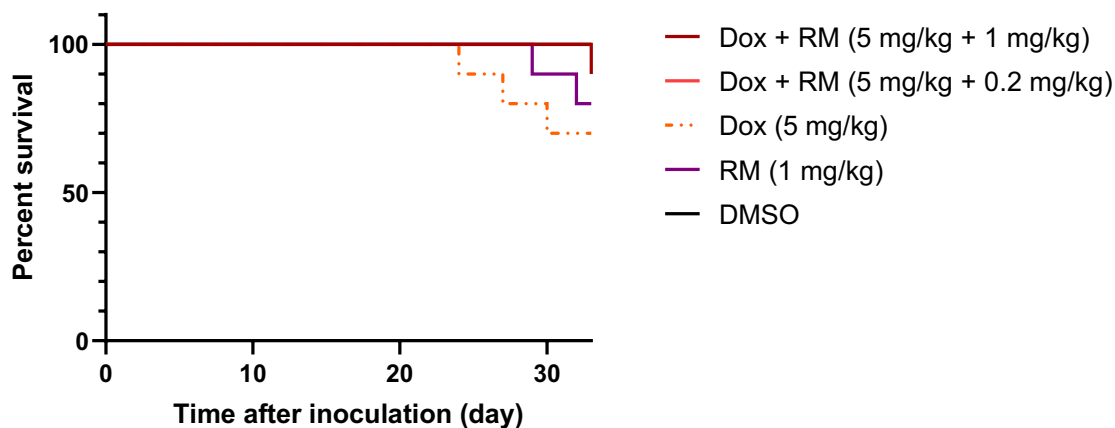


Figure 4: Kaplan-Meier survival analysis of 4T1-injected treated and untreated mice.

Histopathology analysis: Hematoxylin and Eosin staining

To compare the histopathological changes in untreated and treated 4T1 challenged mice, tumor, liver, and lung tissues were harvested at day 35, fixed, and stained with hematoxylin and eosin (H&E) (Figure 5). H&E staining can accurately identify tumor regions and invasive metastases. It requires immobilized sections of the sample and is suitable for *ex vivo* pathological analysis. Here, H&E staining was used to quantify the metastatic regions in both the liver and lung tissues to provide insights into the anti-metastatic effects of the single and combination treatments. 4T1-injected mice showed lesions as revealed by condensed apoptotic nuclei, nuclei segmentation and hyperchrome prominent nucleoli, which were all identified indicators of metastatic infiltrations (Jørgensen et al. 2017; Li et al. 2018; Shovon et al. 2022; Valkonen et al. 2017). We used the divergent cell nuclei features from whole slide imaging and

quantified the region of interest using ImageJ software (Schneider et al. 2012) (Figure 6). Quantitation of the metastatic infiltrations in the liver tissue revealed a significant reduction in treated groups compared to untreated groups. When compared to each treatment type, the combination setups showed the most promising reduction in metastases with the Dox + RM (5 mg/kg + 1 mg/kg) as the most effective treatment with an average reduction of 83.63% compared to the untreated group. This was followed closely by the single RM dose (2 mg/kg) and combination Dox + RM (5mg/kg + 0.2 mg/kg) at 76.04% and 75.33%, respectively. The rest of the percentage reduction in liver metastases of the different treatments is listed in Table 1. On the other hand, the quantification of lung metastases showed equivocal findings due to uneven lung tissue sectioning and hard-to-identify congested lung tissues and large cancer infiltrations.

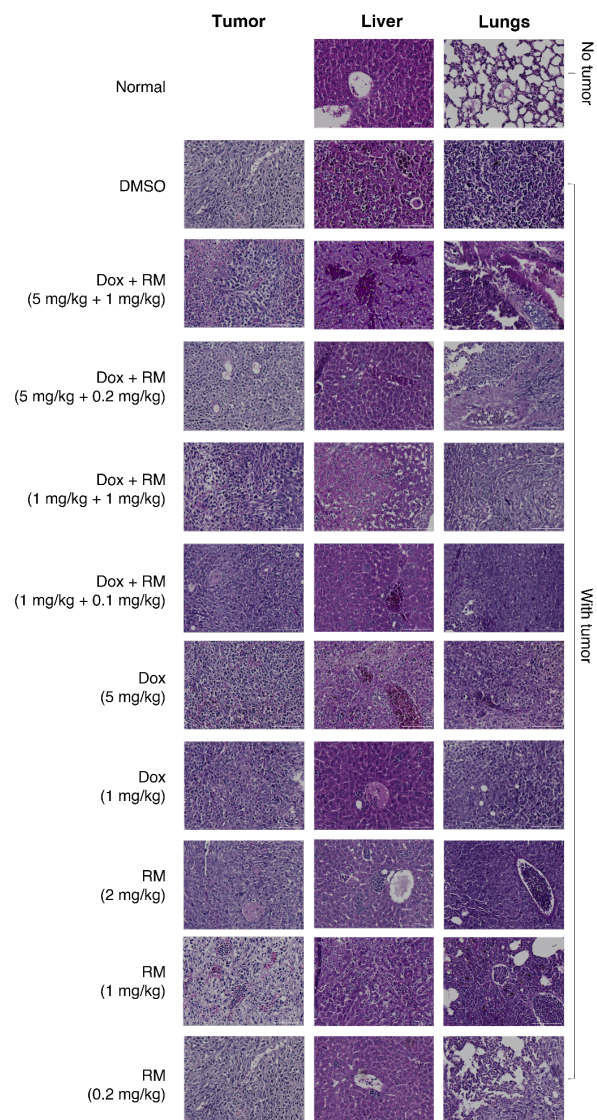


Figure 5: Hematoxylin and eosin (H&E) staining of tumor, liver, and lung slices from untreated and treated 4T1-injected mice (20x magnification viewed under an Olympus IX70 inverted microscope captured using CellSens software).

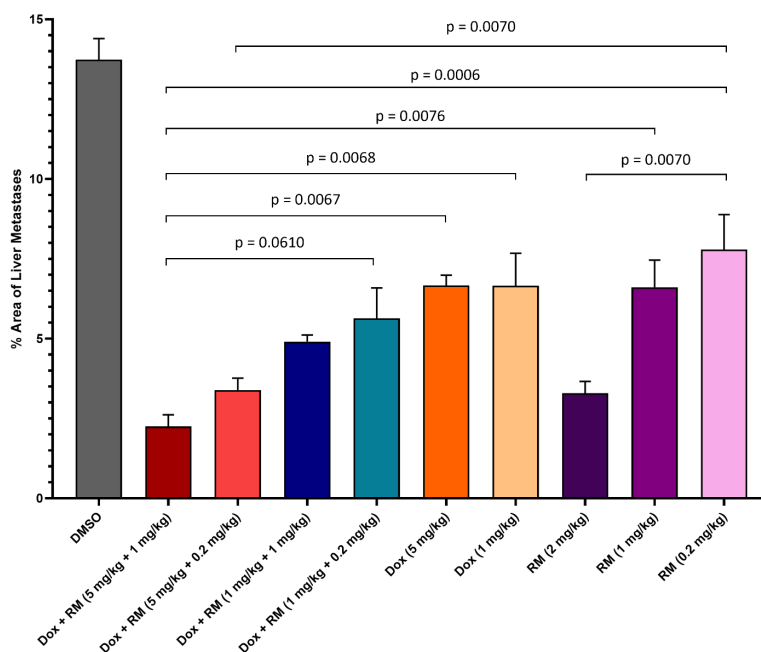


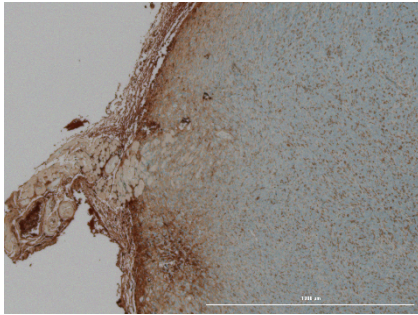
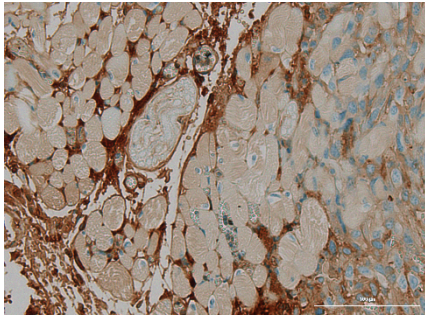
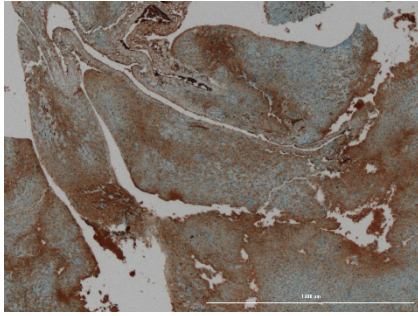
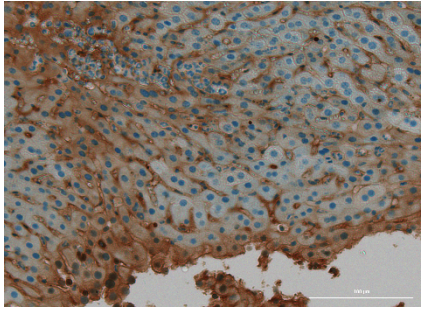
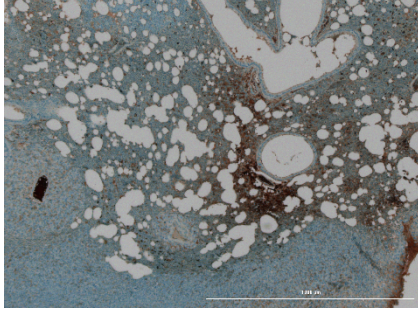
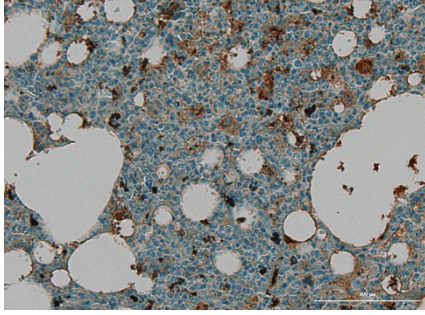
Figure 6: Metastatic infiltration quantified from the H&E staining of liver samples (20x). Regions of interest were identified based on the appearance of divergent nuclei segmentation and hyperchrome nucleoli. Quantitation was in whole slice imaging analysis using ImageJ software. Bars represent the mean + SEM, (each treatment has three slides) and lines above the means indicate significant differences among treatments. All treatments are significantly different relative to the DMSO control (ANOVA and Tukey's multiple comparison test; $P < 0.05$).

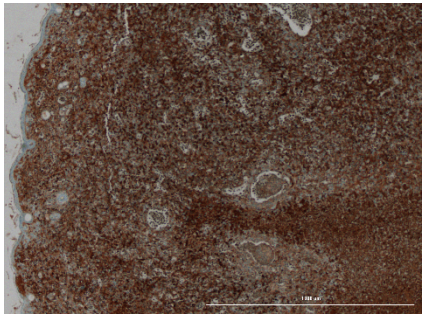
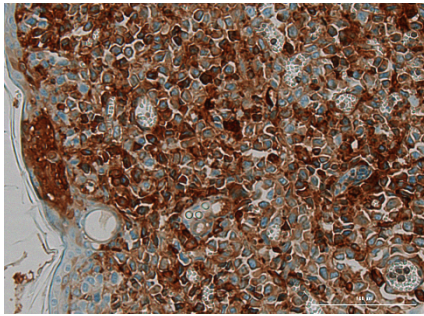
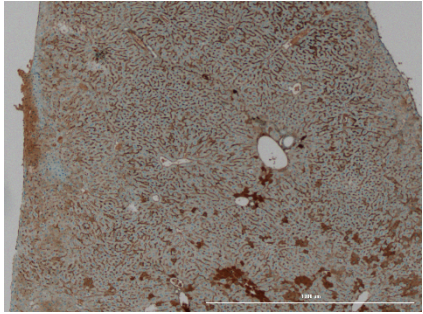
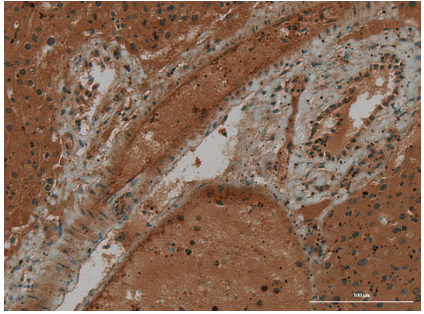
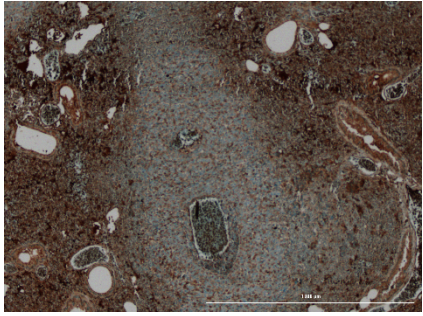
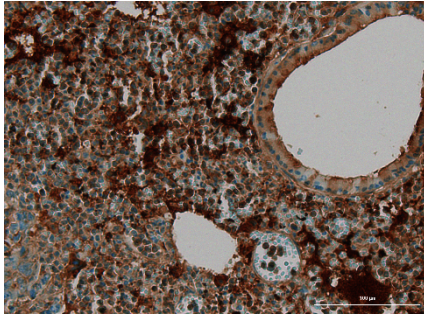
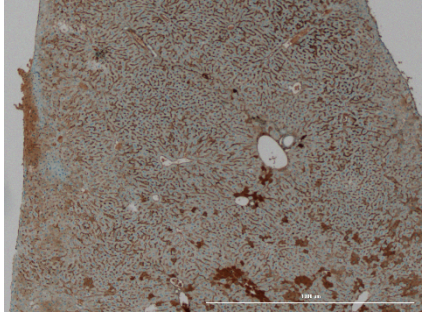
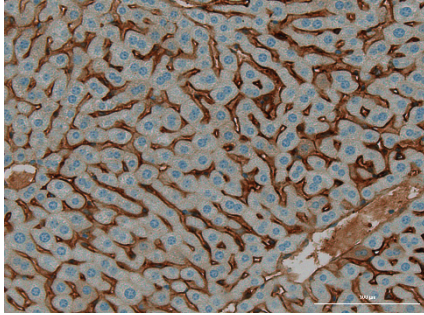
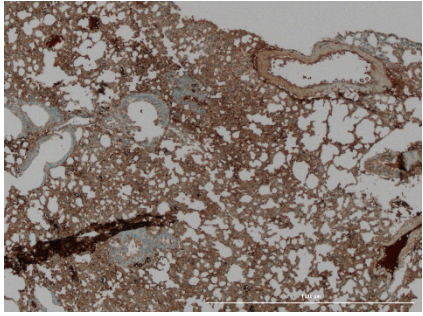
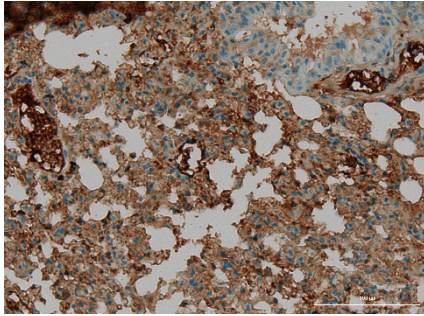
Table 1: Percent reduction in liver metastases relative to DMSO control-treated animals

Treatment (dosage)	Percent Reduction
Dox + RM (5 mg/kg + 1 mg/kg)	83.63 ± 3.77
Dox + RM (5 mg/kg + 0.2 mg/kg)	75.33 ± 3.88
Dox + RM (1 mg/kg + 1 mg/kg)	64.26 ± 2.09
Dox + RM (1 mg/kg + 0.2 mg/kg)	58.95 ± 9.76
Dox (5 mg/kg)	51.46 ± 3.31
Dox (1 mg/kg)	51.52 ± 10.46
RM (2 mg/kg)	76.04 ± 3.83
RM (1 mg/kg)	51.87 ± 8.74
RM (0.2 mg/kg)	43.31 ± 11.29

Immunohistochemistry analysis using p63 marker

Table 2: p63 Immunohistochemistry (IHC) staining of the tumor, liver, and lung sections from the Dox + RM (5 mg/kg + 1 mg/kg), vehicle control group, and normal (non-treated, no-tumor) group at 4X and 20X magnifications. The expression of p63 is indicated by the brown stains. (4X and 20X magnification viewed under an Olympus IX70 inverted microscope captured using CellSens software).

Set up	organ/tissue	4X	20X
Dox + RM (5 mg/kg + 1 mg/kg)	Tumor		
	Liver		
	Lungs		

Vehicle control	Tumor		
	Liver		
	Lungs		
Normal cell (4T1-negative setup)	Liver		
	Lungs		

The transcription factor tumor protein 63 (p63) belongs to the p53 gene family which plays an important role in cellular differentiation and carcinogenesis (Dötsch et al. 2010; Westfall and Pietenpol 2004). High expression of p63 in different cell and tissue types enables its use in immunohistochemistry (IHC) as a cell marker for cancer diagnosis in different glands and tissues, including the breasts (Steurer et al. 2021; Westfall and Pietenpol 2004). In this study, tissue samples of varying treatments were

selected for p63 IHC. The p63 IHC staining analysis of the tumor, liver, and lungs from the Dox + RM (5 mg/kg + 1 mg/kg), vehicle control, and normal setup (no tumor) were conducted by the affiliated pathologist of Hi-Precision Diagnostics (Table 2). All the stained tissues in Dox + RM (5 mg/kg + 1 mg/kg) showed positive p63 expression in neoplastic cells wherein p63 positive myoepithelial cells were detected in the tumor while metastasis of mammary carcinoma was observed in the liver and the lungs.

Poor p63 uptake in some areas of interest and non-specific staining were also reported in the lungs and liver. For the vehicle control group, tumor and lungs were positive for p63 expression and showed metastatic mammary carcinoma. The lung tissue, on the other hand, showed non-specific staining in much of the liver parenchyma. The normal (non-treated, no-tumor control group) setup resulted in unexpected observations wherein positive p63 expression with non-specific stains in some areas of the liver was detected, while poor uptake of p63 was reported for the lungs. Notably, as seen in Table 2, lower intensity of the staining can be observed for all the tissues, especially the lungs in the treated group in comparison to the non-treated groups indicating

reduced p63 expression (intensity profiles data using CellSens software not shown). This suggested the combinatorial treatment of Dox and RM may exhibit an effect on the tumor and metastasis of the carcinoma. Further validation and analysis are needed to verify these observations.

Assessment of treatment toxicities

In silico Absorption, Distribution, Metabolism, Excretion, Toxicity (ADMET) of RM

Table 3: Tabulated in silico ADMET of RM from pkCSM

Property		Predicted value	Reference value*
ABSORPTION	Water solubility	-3.739 log mol/L	
	Caco2 permeability	0.39 log Papp in 10 ⁻⁶ cm/s	Papp > 8 x 10 ⁻⁶ cm/s
	Intestinal absorption (human)	79.557% absorbed	> 30%
	Skin permeability	-2.772 log Kp	log Kp < -2.5
	P-glycoprotein substrate	Yes	
	P-glycoprotein I inhibitor	Yes	
	P-glycoprotein II inhibitor	No	
DISTRIBUTION	VDss (human)	-0.49 log L/kg	-0.15 (low) > VDss > 0.45 (high)
	Fraction unbound (human)	0.532 log L/kg	
	BBB permeability	-1.194 log BB	log BB > 0.3
	CNS permeability	-3.478 log PS	log > -2
METABOLISM	CYP2D6 substrate	No	
	CYP3A4 substrate	Yes	
	CYP1A2 inhibitor	No	
	CYP2C19 inhibitor	No	
	CYP2C9 inhibitor	No	
	CYP2D6 inhibitor	No	
	CYP3A4 inhibitor	No	
EXCRETION	Total clearance	0.766 log mL/min/kg	
	Renal OCT2 substrate	No	
TOXICITY	AMES toxicity	No	
	Max. tolerated dose (human)	-0.535 log mg/kg/day	0.477 (low) > MRTD > 0.477 (high)
	hERG I inhibitor	No	
	hERG II inhibitor	No	
	Oral Rat Acute Toxicity (LD50)	3.053 mol/kg	
	Oral Rat Chronic Toxicity (LOAEL)	1.916 log mg/kg/bw/day	
	Hepatotoxicity	Yes	
	Skin sensitization	No	

	<i>T. pyriformis</i> toxicity	0.285 log ug/L	> -0.5 log ug/L (toxic)
	Minnow toxicity	2.271 log mM	LC50 < 0.5 (high acute toxicity)

*Reference values were lifted from the Theory Tab on how to interpret the results in the pkCSM web server (<https://biosig.lab.uq.edu.au/pkcsm>)

Due to the observed protective functions of the combination treatments and the known cytotoxicity of doxorubicin, we performed *in silico* ADMET analysis on RM to provide insights on the pharmacokinetics-pharmacodynamics and assess its contribution to drug toxicity. The ADMET properties of RM based on its structure were predicted using the free web server pkCSM (Pires et al. 2015). The prediction showed low Caco2 permeability and high intestinal absorption, indicating that the compound is not readily absorbed by the colon if orally administered but a proportion of the compound is readily absorbed through the human small intestine. RM is also skin-permeable and has no skin sensitization which means it has no adverse effect when applied dermally; hence, it can be developed for transdermal drug delivery. It can be transported by P-glycoprotein (P-gp) and can also inhibit P-gp I transport. A low volume of RM is also needed for the total dose to be uniformly distributed to give the same concentration in the blood plasma. RM was also predicted to have a weak ability to cross into the blood brain barrier and to penetrate the central nervous system. In terms of metabolism, RM can be metabolized and biotransformed by cytochrome CYP3A4 but not CYP2D6 suggesting specificity with a cytochrome isoform. Moreover, it does not inhibit cytochrome P450 suggesting that it does not compete with other drugs for the enzymes. The predictor showed that RM is not a renal OCT2 substrate; thus, it cannot be transported by the protein which is important for renal clearance and potential contraindications. The compound was also predicted to have no mutagenic potential based on the AMES test and has a low toxic dose threshold in humans. It also does not inhibit potassium channels encoded by hERG. Based on toxicity prediction, RM can cause disruption in the normal function of the liver and is toxic against *T. pyriformis* and Flathead Minnows. This *in silico* ADME toxicity assessment will be supplemented with pharmacokinetic (PK) measurements in the future.

CONCLUSION

In summary, our study revealed promising results regarding the efficacy of the doxorubicin (Dox) and renieramycin M (RM) combination in slowing down breast cancer tumor progression in a murine model. Tumor volume measurements and histopathological analyses using hematoxylin and eosin staining suggest that this combination treatment not only retards tumor growth but also leads to a significant reduction in metastases, particularly when considering quantified metastatic infiltrations in liver tissues.

Although the use of p63 to confirm metastases as breast carcinomas presented some challenges in quantification and analysis, the overall trends in our data support the potential of this drug combination for breast cancer treatment. Furthermore, our research has unveiled an unexpected benefit: a significant delay and decrease in clinical signs of toxicity, as demonstrated through the monitoring of moribundity and animal death. This observation requires further studies to elucidate the causative factors and the underlying synergistic mechanism of action of the combination treatment. These findings underscore the clinical potential of the Dox and RM combination for breast cancer treatment, offering not only enhanced therapeutic efficacy but also a potential reduction in treatment-related adverse effects.

This paper represents the first report of *in vivo* analysis of the Dox and RM combination in breast cancer murine models, providing valuable insights into the potential of combination therapies. The observed synergy has biological and clinical significance, suggesting a promising direction for future clinical development. While additional trials and mechanistic studies are warranted, these findings provide a promising path toward improved therapies, offering a more effective and less toxic approach to mitigating breast cancer. These results not only hold promise for improved breast cancer therapies but also raise important questions and opportunities for further research and development of marine natural products in the quest to combat this challenging disease.

ACKNOWLEDGMENT

This work was funded by the Philippine National Academy of Science and Technology (NAST-PHL) fellowship grant of G.P.C. The US NIH PMS-ICBG grant of G.P.C. and Department of Science and Technology Philippine Council for Health Research and Development funding through the Discovery and Development of Health Products-Marine Component grant of L.A.S.R. provided supplementary support. The authors would like to thank Ma. Suzanneth G. Lola, DVM, MSc for providing her expertise by reading the slides and performing histopathological analyses on selected slides from H&E and p63 IHC staining. This is MSI Contribution No.1598.

CONFLICT OF INTEREST

The authors are filing a patent application for this study.

CONTRIBUTIONS OF INDIVIDUAL AUTHORS

ZGA: conceptualization, methodology, formal analysis, validation, visualization, writing—original draft, writing—review and editing. SRS-G: investigation, methodology, writing—original draft, MRDP: methodology, investigation. ELB: investigation. LAS-R: conceptualization, funding acquisition, methodology, project administration, resources, supervision, writing—original draft, writing—review and editing. GPC: inception, conceptualization, funding acquisition, resources, supervision, writing—original draft, writing—review and editing.

REFERENCES

- Andreopoulou E and Sparano JA. Chemotherapy in patients with anthracycline and taxane-pretreated metastatic breast cancer: An overview. *Current Breast Cancer Reports* 2013; 5(1): 42-50. <https://doi.org/10.1007/s12609-012-0097-1>
- Argenziano M, Gigliotti CL, Clemente N, Boggio E, Ferrara B, Trotta F, Pizzimenti S, Barrera G, Boldorini R, Bessone F, Dianzani U, Cavalli R, Dianzani C. Improvement in the anti-tumor efficacy of doxorubicin nanosponges in *in vitro* and in mice bearing breast tumor models. *Cancers* 2020; 12(1):162. <https://doi.org/10.3390/cancers12010162>

- Arnold M, Morgan E, Rumgay H, Mafra A, Singh D, Laversanne M, Vignat J, Gralow JR, Cardoso F, Siesling S, Soerjomataram I. Current and future burden of breast cancer: Global statistics for 2020 and 2040. *Breast* 2022; 66:15-23. <https://doi.org/10.1016/j.breast.2022.08.010>
- Bao L, Haque A, Jackson K, Hazari S, Moroz K, Jetly R, Dash S. Increased expression of p-glycoprotein is associated with doxorubicin chemoresistance in the metastatic 4T1 breast cancer model. *American Journal of Pathology* 2011; 178(2):838-852. <https://doi.org/10.1016/j.ajpath.2010.10.029>
- Carlson BL, Pokorny JL, Schroeder MA, Sarkaria JN. Establishment, maintenance and in vitro and in vivo applications of primary human glioblastoma multiforme (GBM) xenograft models for translational biology studies and drug discovery. *Current Protocols in Pharmacology* 2011; Chapter 14(14):Unit 14.16. <https://doi.org/10.1002/0471141755.ph1416s2>
- Chamni S, Sirimangkalakitti N, Chanvorachote P, Suwanborirux K, Saito N. Chemistry of renieramycins. Part 19: Semi-syntheses of 22-O-amino ester and hydroquinone 5-O-amino ester derivatives of renieramycin m and their cytotoxicity against non-small-cell lung cancer cell lines. *Marine Drugs* 2020; 18(8):418. <https://doi.org/10.3390/MD18080418>
- Charupant K, Daikuhara N, Saito E, Amnuoyopol S, Suwanborirux K, Owa T, Saito N. Chemistry of renieramycins. Part 8: Synthesis and cytotoxicity evaluation of renieramycin M-jorunnamycin A analogues. *Bioorganic and Medicinal Chemistry* 2009; 17(13): 4548-4558. <https://doi.org/10.1016/j.bmc.2009.05.009>
- Charupant K, Suwanborirux K, Daikuhara N, Yokoya M, Ushijima-Sugano R, Kawai T, Owa T, Saito N. Microarray-based transcriptional profiling of renieramycin M and jorunnamycin C, isolated from Thai marine organisms. *Marine Drugs* 2009; 7(4): 483-494. <https://doi.org/10.3390/md7040483>
- Chatterjee K, Zhang J, Honbo N, Karliner JS. Doxorubicin cardiomyopathy. *Cardiology* 2010; 115(2):155-162. <https://doi.org/10.1159/000265166>
- Dötsch V, Bernassola F, Coutandin D, Candi E, Melino G. (2010). p63 and p73, the ancestors of p53. *Cold Spring Harbor perspectives in biology* 2010; 2(9). <https://doi.org/10.1101/cshperspect.a004887>
- Dudley WN, Wickham R, Coombs N. An introduction to survival statistics: Kaplan-Meier analysis. *Journal of the Advanced Practitioner in Oncology* 2016; 7(1):91-100. <https://doi.org/10.6004/jadpro.2016.7.1.8>
- Dulf PL, Mocan M, Coadă CA, Dulf DV, Moldovan R, Baldea I, Farcas AD, Blendea D, Filip AG. Doxorubicin-induced acute cardiotoxicity is associated with increased oxidative stress, autophagy, and inflammation in a murine model. *Naunyn-Schmiedeberg's Archives of Pharmacology* 2023; 396(6):1105-1115. <https://doi.org/10.1007/s00210-023-02382-z>
- Faustino-Rocha A, Oliveira PA, Pinho-Oliveira J, Teixeira-Guedes C, Soares-Maia R, Da Costa RG, Colaço B, Pires MJ, Colaço J, Ferreira R, Ginja M. Estimation of rat mammary tumor volume using caliper and ultrasonography measurements. *Lab Animal* 2013; 42(6):217-224. <https://doi.org/10.1038/labana.254>
- Gamucci T, D'Ottavio AM, Magnolfi E, Barduagni M, Vaccaro A, Sperduti I, Moscetti L, Belli F, Meliffi L. Weekly epirubicin plus docetaxel as first-line treatment in metastatic breast cancer. *British Journal of Cancer* 2007; 97(8):1040-1045. <https://doi.org/10.1038/sj.bjc.6603982>
- Gogate A, Wheeler SB, Reeder-Hayes KE, Ekwueme DU, Fairley TL, Drier S, Trogdon JG. Projecting the prevalence and costs of metastatic breast cancer from 2015 through 2030. *JNCI Cancer Spectrum* 2021; 5(4): pkab063. <https://doi.org/10.1093/jncics/pkab063>
- Halim H, Chunhacha P, Suwanborirux K, Chanvorachote P. Anticancer and antimetastatic activities of renieramycin M, a marine tetrahydroisoquinoline alkaloid, in human non-small cell lung cancer cells. *Anticancer Research* 2011; 31(1):193-201. <http://ar.iiarjournals.org/content/31/1/193.abstract>
- Jørgensen AS, Rasmussen AM, Andersen NKM, Andersen SK, Emborg J, Røge R, Østergaard LR. Using cell nuclei features to detect colon cancer tissue in hematoxylin and eosin stained slides. *Cytometry Part A* 2017; 91(8):785-793. <https://doi.org/10.1002/cyto.a.23175>
- Li Y, Li N, Yu X, Huang K, Zheng T, Cheng X, Zeng S, Liu X. Hematoxylin and eosin staining of intact tissues via delipidation and ultrasound. *Scientific Reports* 2018; 8:12259. <https://doi.org/10.1038/s41598-018-30755-5>
- Mariotto AB, Yabroff KR, Shao Y, Feuer EJ, Brown, ML. Projections of the cost of cancer care in the United States: 2010-2020. *Journal of the National Cancer Institute* 2011; 103(2): 117-128. <https://doi.org/10.1093/jnci/djq495>
- Meco D, Colombo T, Ubezio P, Zucchetti M, Zaffaroni M, Riccardi A, Faircloth G, Jose J, D'Incalci M, Riccardi R. Effective combination of ET-743 and doxorubicin in sarcoma: Preclinical studies. *Cancer Chemotherapy and Pharmacology* 2003; 52(2):131-138. <https://doi.org/10.1007/s00280-003-0636-6>
- Mishima H, Kato T, Yanagisawa M, Tsujinaka T, Nishisho I, Tsujie M, Fujimoto-Ouchi K, Tanaka Y, Kikkawa N. Sequential treatment with irinotecan and doxifluridine: Optimal dosing schedule in murine models and in a phase I study for metastatic colorectal cancer. *Chemotherapy* 2005; 51(1): 32-39. <https://doi.org/10.1159/000084416>
- Mosmann T. Rapid colorimetric assay for cellular growth and survival: application to proliferation and cytotoxicity assays. *Journal of immunological methods* 1983; 65(1-2): 55-63. [https://doi.org/10.1016/0022-1759\(83\)90303-4](https://doi.org/10.1016/0022-1759(83)90303-4)
- Pires DEV, Blundell TL, Ascher DB. pkCSM: Predicting small-molecule pharmacokinetic and toxicity properties using graph-based signatures. *Journal of Medicinal Chemistry* 2015; 58(9):4066-4072. <https://doi.org/10.1021/acs.jmedchem.5b00104>
- Pulaski BA and Ostrand-Rosenberg S. Reduction of established spontaneous mammary carcinoma metastases following immunotherapy with major histocompatibility complex Class II and B7.1 Cell-based Tumor Vaccines1. *Cancer Research* 1998;58(7):1486-93. <http://aacrjournals.org/cancerres/article-pdf/58/7/1486/2469218/cr0580071486.pdf>
- Saito N, Tanaka C, Koizumi YI, Suwanborirux K, Amnuoyopol S, Pummangura S, Kubo, A. Chemistry of renieramycins. Part 6: Transformation of renieramycin M into jorumycin and renieramycin J including oxidative degradation products,

- mimosamycin, renierone, and renierol acetate. *Tetrahedron* 2004; 60(17): 3873-3881. <https://doi.org/10.1016/j.tet.2004.02.071>
- Santiago VS, Manzano GG, Yu CC, Aliño PM, Salvador-Reyes LA. Mariculture potential of renieramycin-producing Philippine blue sponge *Xestospongia* sp. (Porifera: Haplosclerida). *Aquaculture* 2019; 502:356-364. <https://doi.org/10.1016/j.aquaculture.2018.12.059>
- Sápi J, Kovács L, Drexler DA, Kocsis P, Gajári D, Sápi Z. Tumor volume estimation and quasi-continuous administration for most effective bevacizumab therapy. *PLOS One* 2015; 10(11):1-20. <https://doi.org/10.1371/journal.pone.0142190>
- Sewell F, Ragan I, Marczylo T, Anderson B, Braun A, Casey W, Dennison N, Griffiths D, Guest R, Holmes T, van Huygevoort T, Indans I, Kenny T, Kojima H, Lee K, Prieto P, Smith P, Smedley J, Stokes W, Wnorowski G, Horgan G. A global initiative to refine acute inhalation studies through the use of “evident toxicity” as an endpoint: Towards adoption of the fixed concentration procedure. *Regulatory Toxicology and Pharmacology* 2015; 73(3):770-779. <https://doi.org/10.1016/j.yrtph.2015.10.018>
- Schneider C, Rasband W, Eliceiri, K. NIH Image to ImageJ: 25 years of image analysis. *Nature Methods* 2012; 9:671–675. <https://doi.org/10.1038/nmeth.2089>
- Shovon MSH, Islam MJ, Nabil MNAK, Molla MM, Jony AI, Mridha MF. Strategies for enhancing the multi-stage classification performances of HER2 breast cancer from hematoxylin and eosin images. *Diagnostics* 2022; 12(11):2825. <https://doi.org/10.3390/diagnostics12112825>
- Steurer S, Riemann C, Büscheck F, Luebke AM, Kluth M, Hube-Magg C, Hinsch A, Höflmayer D, Weidemann S, Fraune C, Möller K, Menz A, Fisch M, Rink M, Bernreuther C, Lebok P, Claudit TS, Sauter G, Uhlig R, Wilczak W, Dum D, Simon R, Minner S, Burandt E, Krech R, Krech T, Marx AH. p63 expression in human tumors and normal tissues: a tissue microarray study on 10,200 tumors. *Biomarker Research* 2021; 9(1):7. <https://doi.org/10.1186/s40364-021-00260-5>
- Suwanborirux K, Amnuoyopol S, Plubrukarn A, Pummangura S, Kubo A, Tanaka C, Saito N. Chemistry of renieramycins. Part 3. Isolation and structure of stabilized renieramycin type derivatives possessing antitumor activity from Thai sponge *Xestospongia* species, pretreated with potassium cyanide. *Journal of Natural Products* 2003; 66(11):1441-1446. <https://doi.org/10.1021/np030262p>
- Tun, JO, Salvador-Reyes LA, Velarde MC, Saito N, Suwanborirux K, Concepcion GP. (2019). Synergistic cytotoxicity of renieramycin M and doxorubicin in MCF-7 breast cancer cells. *Marine Drugs* 2019; 17(9):1-26. <https://doi.org/10.3390/md17090536>
- Valkonen M, Kartasalo K, Liimatainen K, Nykter M, Latonen L, Ruusuvauro P. Metastasis detection from whole slide images using local features and random forests. *Cytometry Part A* 2017; 91(6):555-565. <https://doi.org/10.1002/cyto.a.23089>
- Westfall MD and Pietenpol JA. p63: Molecular complexity in development and cancer. *Carcinogenesis* 2004; 25(6):857-864. <https://doi.org/10.1093/carcin/bgh148>
- Yamagishi T, Kawano M, Watanabe H, Yagi A, Shintaku Y, Ohno K, Yamamoto H. Severity Classification of clinical signs and defining the moribund state as an experimental endpoint for acute toxicity testing using Japanese Medaka (*Oryzias latipes*). *Environmental Toxicology and Chemistry* 2022; 41(4):1089-1095. <https://doi.org/10.1002/etc.5294>
- Zheng R, Han S, Duan C, Chen K, You Z, Jia J, Lin S, Liang L, Liu A, Long H, Wang S. Role of taxane and anthracycline combination regimens in the management of advanced breast cancer: a meta-analysis of randomized trials. *Medicine (United States)* 2014; 94(17): e803. <https://doi.org/10.1097/MD.0000000000000803>

SUPPLEMENTARY INFORMATION

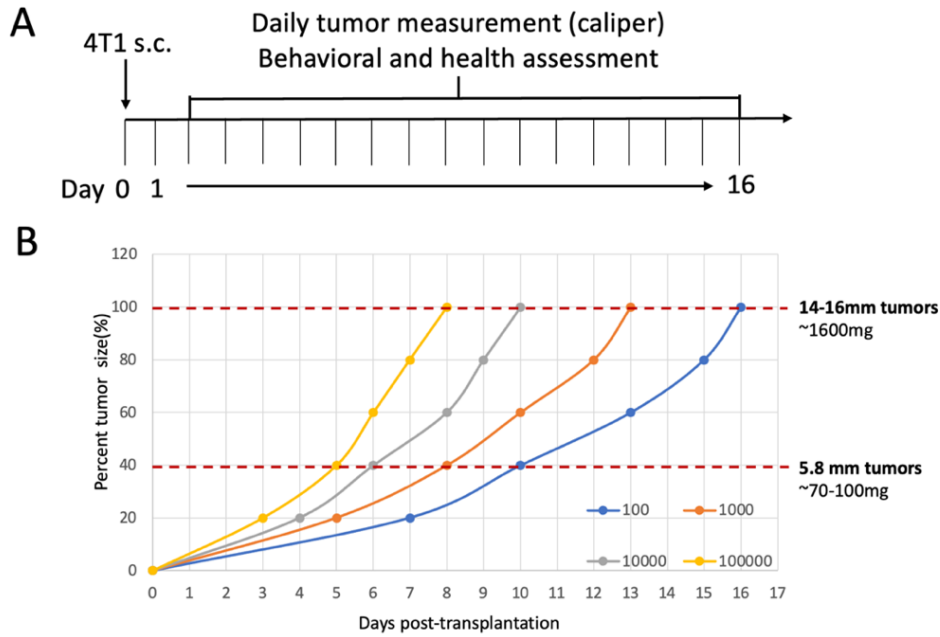


Figure S1: Optimization of 4T1 cell number for inoculation. A) Schematic diagram of timeline of inoculation and measurement, (n = 4). B) Tumor volume and experimental protocol from day 0 to end point day 17 of all treatment setup. The rate of tumor growth in observed palpable tumors was determined in 100, 1000, 10000, and 100000 inoculated 4T1 cells.

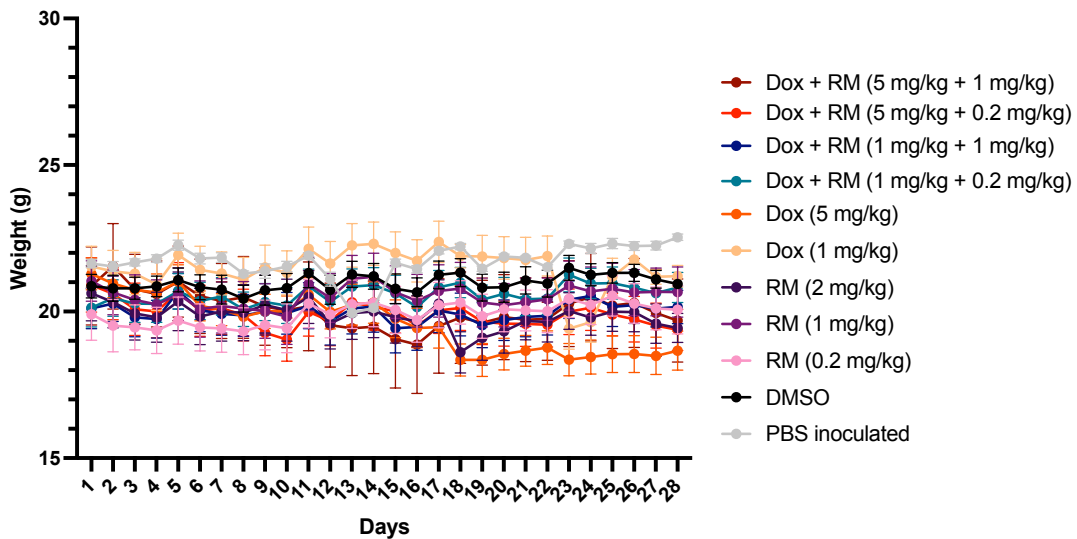


Figure S2: Daily recorded weights of mice. Mice were weighted every day at around 2 pm using a standard portable balance. No significant difference between setups was found.

Table S1: Number of mice used in experimental setups from trial 1 and trial 2

Treatment (dose)	Number of mice used	
	Trial 1 ^a	Trial 2 ^b
Dox + RM (5 mg/kg + 1 mg/kg)	4	6
Dox + RM (5 mg/kg + 0.2 mg/kg)	4	6
Dox + RM (1 mg/kg + 1 mg/kg)	4	6
Dox + RM (1 mg/kg + 0.2 mg/kg)	4	6
Dox (5 mg/kg)	4	6
Dox (1 mg/kg)	4	6
RM (2 mg/kg)	0	6
RM (1 mg/kg)	4	6
RM (0.2 mg/kg)	4	6

^a 1 mouse was identified as outlier per setup using IQR

^b 2 mice were identified as outliers per setup using IQR